Temporal patterns and ~~potential~~ drivers of CO_2 emission from dry sediments in a groyne field of a large river

Matthias Koschorreck[1], Klaus Holger Knorr[2], Lelaina Teichert[1,2]

[1]Department of Lake Research, Helmholtz Centre for Environmental Research – UFZ, Magdeburg, 39114, Germany
[2]Institute of Landscape Ecology, Westfälische Wilhelms-University, Münster, Germany

Correspondence to: Matthias Koschorreck (Matthias.koschorreck@ufz.de)

Abstract. River sediments falling dry at low water level are sources of CO_2 to the atmosphere. While the general relevance of CO_2 emissions from dry sediments has been acknowledged and some regulatory mechanisms identified, knowledge on mechanisms and temporal dynamics is still sparse. Using a combination of high frequency measurements and detailed studies we thus aimed to identify processes responsible for CO_2 emissions and to assess temporal dynamics of CO_2 emissions from dry sediments at a large German river.

CO_2 emissions were largely driven by microbial respiration in the sediment. Observed CO_2 fluxes could be explained by patterns and responses of sediment respiration rates measured in laboratory incubations. We exclude groundwater as a significant source of CO_2 because potential evaporation rates were too low to explain CO_2 fluxes by groundwater evaporation. Furthermore, CO_2 fluxes were not related to radon fluxes, which we used to trace groundwater derived degassing of CO_2.

CO_2 emissions were strongly regulated by temperature resulting in large diurnal fluctuations of CO_2 emissions with emissions peaking during the day. The diurnal temperature – CO_2 flux relation exhibited a hysteresis which highlights the effect of transport processes in the sediment and makes it difficult to identify temperature dependence from simple linear regressions. The temperature response of CO_2 flux and sediment respiration rates in laboratory incubations was identical. Also deeper sediment layers apparently contributed to CO_2 emissions because the CO_2 flux was correlated with the thickness of the unsaturated zone, resulting in CO_2 fluxes increasing with distance to the local groundwater level and with distance to the river. Rain events lowered CO_2 emissions from dry river sediments probably by blocking CO_2 transport from deeper sediment layers to the atmosphere. Terrestrial vegetation growing on exposed

sediments greatly~~largely~~ increased respiratory sediment CO_2 emissions. We conclude ~~show~~ that the regulation of CO_2 emissions from dry river sediments is complex. Diurnal measurements are mandatory

30 and even CO_2 uptake in the dark by phototrophic micro-organisms has to be considered when assessing the impact of dry sediments on CO_2 emissions from rivers.

1 Introduction

1.1 CO_2 emissions from dry river sediments – significance

Streams and rivers are well known to play an important role in the global carbon cycle. The transport of

35 continental carbon to the ocean is mainly regulated by rivers (Schlesinger and Melack 1981). Moreover, carbon in rivers undergoes transformation processes and can be stored by means of sedimentation and photosynthesis or released due to biological respiration (Battin et al. 2009). One distinctive feature of rivers is their frequently changing water level~~s~~. Climate change is expected to further increase the seasonal and the inter-annual variability of rivers and hydrological regimes (Bolpagni et al. 2019; Coppola et al.

40 2014). In Europe, more frequent and longer-lasting droughts are expected during summers, which lead to low water levels in~~desiccation of smaller~~ streams and ~~low water levels in high order~~ rivers (Spinoni et al. 2018). Consequently, previously submerged river sediment will be exposed to the atmosphere and influenced by drying (Steward et al. 2012). It has been shown that these exposed sediments can emit high amounts of CO_2 (von Schiller et al. 2014) and may represent a globally relevant carbon source to the

45 atmosphere (Marcé et al. 2019).

1.2 Regulation of CO_2 emissions from dry sediments

While the relevance of CO_2 emissions from dry river sediments has been acknowledged, only little is known about underlying mechanisms and temporal patterns. A recent study identified organic matter content and moisture as common drivers of CO_2 emissions from dry aquatic sediments (Keller et al. 2020).

50 However, high variability prevents the prediction of CO_2 fluxes for particular sites. Case studies showed that CO_2 emissions are affected by temperature (Doering et al. 2011), emergent vegetation (Bolpagni et al. 2017), organic matter (Palmia et al. 2021), water content (Martinsen et al. 2019), or the frequency of

dry-wet cycles (Machado dos Santos Pinto et al. 2020). Although it is known that CO_2 emission from dry sediment may change with time, existing studies are based on single or few measurements. Few studies did address temporal variability of CO_2 emissions, but ~~N~~nothing is yet known about short term dynamics of GHG emissions from dry aquatic sediments. Investigating temporal variability of CO_2 fluxes should provide information about the potential sources of emitted CO_2. Knowing sources of emitted CO_2 from dry sediments is crucial to be able to model or scale up GHG emissions from these systems. ~~Investigating temporal variability has the potential to gain knowledge about the sources of emitted CO_2 and will improve our ability to model or scale up GHG emissions from dry sediments.~~

1.3 Possible sources of CO_2

Carbon emissions from desiccated sediments derive from a number of possible biotic and abiotic sources (Marcé et al. 2019). Microbial respiration is well known to contribute to CO_2 emissions (Weise et al. 2016), similar to soil respiration. Organic matter originating from organic particle sedimentation may be mineralized to CO_2 or CH_4. It is typically observed that CH_4 emissions from dry sediments are low indicating that anaerobic mineralization plays a minor role (Marcé et al. 2019).

In contrast to respiration, abiotic processes are rarely taken into account as sources of CO_2 (Rey 2015). Yet, recent findings revealed a spatial variability of CO_2 fluxes from dry river sediments with highest fluxes near to the river ~~at groundwater seeping sites that raised the question, how abiotic processes might contribute to observed CO_2 emissions. As a result,~~ (Mallast et al. 2020). As a possible explanation the authors hypothesize that at decreasing river water level a groundwater flow gradient towards the river would transport groundwater to the river (Peters et al. 2006). Groundwater is usually 10 to 100 fold super-saturated with CO_2 (Macpherson 2009). Near to the river the thickness of the unsaturated layer approaches zero and CO_2 rich groundwater reaches the surface sediment were CO_2 would eventually degas~~suggested that CO_2 evasion from groundwater is likely to contribute to CO_2 emissions from dry river sediments. This hypothesis is based on the mechanism that during periods of desiccation the water level of the river is falling, while the response of the groundwater level is delayed (Peters et al. 2006). Hence, a flow gradient towards the river is established, resulting in discharge hotspots of groundwater close to the river. Considering that groundwater is usually 10 to 100 fold over-saturated with CO_2 (Macpherson 2009) the~~

80 ~~dissolved CO_2 can be expected to degas when reaching the sediment-atmosphere interface and probably~~ ~~adds to the CO_2 emissions~~ (Mallast et al. 2020).

1.4 Aim of study

Given the uncertainty of the origin of CO_2 emitted from dry river sediments, in this study we aimed to test the hypothesis of (Mallast et al. 2020) that CO_2 emissions from dry sediments of larger rivers are

85 driven by groundwater degassing. If groundwater was a significant source of CO2 we hypothesize a only weak temperature dependence of CO_2 emissions. We applied a combination of automatic high frequency measurements and detailed studies using a variety of methods to identify the source of CO_2 emissions from dry sediments at a large German river and to understand their temporal dynamics and drivers.

2 Material and Methods

90 ## 2.1 Study site

The study was conducted at the lowland part of river Elbe, one of the largest rivers in Central Europe with a discharge average of about 559 m^3 s^{-1} at the city of Magdeburg (Weigold and Baborowski 2009). Near Magdeburg, the Middle Elbe can be characterized as a free-flowing lowland river with comparable large floodplains, only regulated by groyne fields. Such groyne fields are the dominant shore type along the

95 German part of the river (Bussmann et al. 2022).

Hence, seasonal water level fluctuations are shaping the different habitats alongside the river, ranging from alluvial forests and pastures to sandy beaches (Scholten et al. 2005). The study site is located near the farm "Apfelwerder" at river km 314 in between two groins and is characterized by a slight slope from the river to the adjoining pasture (52.038398 N, 11.715495 E). Groynes extended about 50 m into the

100 river and distance between groynes was 130±37 m. A sandy beach of about 2 to 5 m with sparse vegetation (*Persicaria lapathifolia, Rorippa amphibia, Polygonum aviculare*) could be found directly at the river, while the vegetation became denser with distance to the river (~~figure~~ Figure S1).

2.2 High frequency measurements

2.2.1 Automatic flux chambers, water table levels, and environmental data

105 To cover the temporal dynamics of CO_2 fluxes three opaque automatic chambers (CFLUX-1 Automated Soil CO_2 Flux System, PP Systems, Amesbury, Massachusetts, USA), were installed (Figure S1a). The chambers measured CO_2 fluxes once every hour. Each flux measurement lasted 5 minutes and between flux measurements the chambers were open for 55 min~~The chambers measured hourly CO_2 fluxes~~. ~~Between flux measurements the chambers were open.~~ CO_2 fluxes were calculated from the linear increase

110 of CO_2 during a closure time of 5 minutes. Each chamber was equipped with a soil moisture and temperature probe (Stevens HydraProbe, Stevens Water Monitoring Systems, Portland, Oregon, USA). Due to fluctuating water levels over the summer of 2020 (Figure 1), it was not possible to measure CO_2 fluxes from the sediment continuously over the whole measurement period. The chambers were set up in the periods from May 1st to June 10th, from August 3rd to August 6th, and from September 17th to

115 September 26th; moreover, also during deployment they needed to be moved occasionally. Automatic flux chamber data were discarded when the collar was flooded or the sand was washed away by waves removed, which resulted in CO_2 concentrations fluctuating around ambient concentration~~Automatic flux chamber data were quality checked and data when the collar was flooded or the sand was washed away by waves removed~~. The final dataset contained 3128 flux measurements.

120 To assure reproducibility and comparability of the automatically measured data, we installed the chambers at defined heights above the gauge "Magdeburg Strombrücke". Therefore, the distance to the river and the height over water level were determined once, along a transect. Out of these parameters, a slope was calculated and afterward used to position the automatic chambers in the field. Positions, where the automatic chambers were placed were 75, 85 and 95 cm above zero point of the gauge "Magdeburg

125 Strombrücke" (located 13 km downstream of the study side, zero point of gauge = 39.885 m above mean sea level (WSV 2020)). The thickness of the unsaturated sediment was calculated as the difference between the height above zero gauge for each chamber and the actual river level. Weather data from the German Weather Service were obtained for the monitoring station Magdeburg 15 km from Apfelwerder (DWD 2020).

130
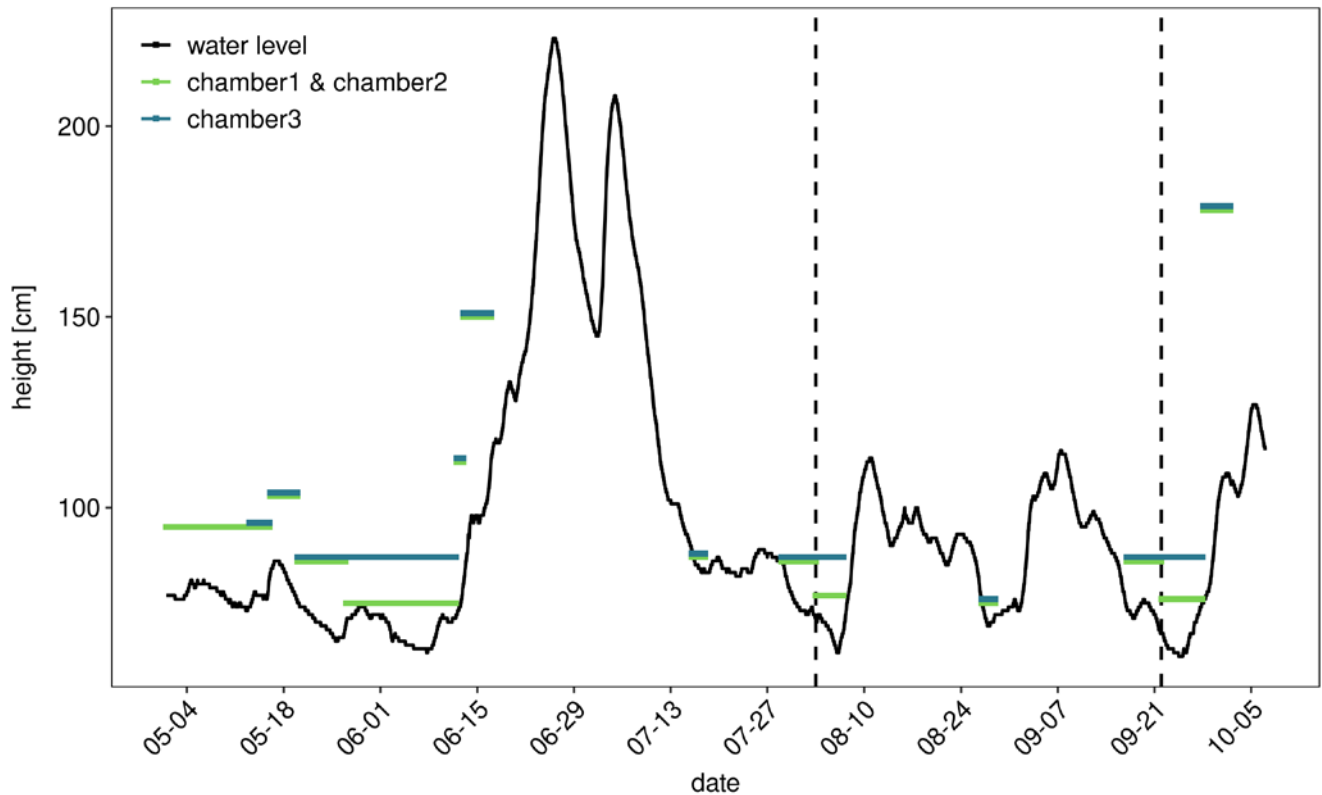
Figure 1: Water level of the Elbe River at gauge "Magdeburg Strombrücke" (12 km downstream) in summer 2020. Colored lines indicate positioning of automatic flux chambers. For example a horizontal line at 95 cm means that a particular chamber was located at the water line when the gauge recorded a water level of 95 cm. Vertical dotted lines indicate intensive sampling campaigns.

2.2.2 High resolution sediment respiration flux transects

135 To investigate spatial variability, ~~On 11 occasions~~ between May and September transects of sediment respiration were ~~additionally~~ measured with a portable soil respiration system (EGM-5 Portable CO_2 Gas Analyser + SRC, PP Systems, Amesbury, Massachusetts, USA) equipped with the same soil moisture and temperature probe as the automatic chambers. On each occasion 12 flux measurements along a 15m long transect from the water upslope were recorded. The opaque chamber was place on vegetation free spots

140 to make sure that sediment respiration was measured. At each measuring spot we took note whether plants were growing nearby.

2.3 Detailed sampling campaigns

To closer investigate the mechanisms behind the CO_2 flux two intensive measurement campaigns were carried out on August 4th, 2020, and September 23rd, 2020.

2.3.1 M~~m~~anual chamber measurements

To quantify ~~During these campaigns~~ CO_2 fluxes at different distance to the river and also check for CH_4 emissions, ~~capturing both biotic and abiotic flux components, from the dry river sediments were measured with a~~ manual chamber measurements were done in 1 m steps away from the flowing water, along a transect which was characterized by an uphill slope of ~ 11.5 %. Collars (39 cm diameter) were installed at 4 sites along the transect a day in advance to minimize disturbance during measurements (~~Fig.~~Figure S1b). For flux measurements an opaque chamber (V = 0.0239 m^3, A = 0.1195 m^2) equipped with a pressure vent tube was placed on a collar. The change of concentrations in the chamber was monitored for every 30 s for ~ 5 minutes, with a multicomponent FTIR gas analyser (DX4000, Gasmet Technologies GmbH, Helsinki, Finland). The FTIR gas analyser continuously measures CO_2, CH_4, and Nitrous oxide (N_2O) with an accuracy of $\pm$ 4 ppm CO_2~~< 2% of the measuring range per zero-point calibration interval~~ , $\pm$ 0.1 ppm CH_4 and N_2O (Gasmet Technologies GmbH 2018). Hence, the detection limit of the CO_2 flux was ~2 mmol m^{-2} d^{-1}, while the CH_4 flux was detectable if above 0.12 mmol m^{-2} d^{-1}, and N_2O if above 0.2 mmol m^{-2} d^{-1}. Fluxes were calculated from the linear increase of the respective gas mixing ratio (Gomez-Gener et al. 2015) with time using the R package glimmr (Keller 2020).

2.3.2 Rn sediment efflux measurements

To assess groundwater degassing ^{222}Rn measurements were performed. The geogenic gas ^{222}Rn is a commonly used natural tracer for groundwater influence in aquatic systems and is additionally known as a useful tool to trace the origins of CO_2 (Cook and Herczeg 2000). Therefore, ^{222}Rn concentrations and fluxes were measured with a portable radon detector (RAD7 Radon Detector, DURRIDGE, Billerica, Massachusetts, USA) to determine the groundwater influence on CO_2 fluxes from dry river sediments. The measurements of the RAD7 are based on electrostatic collection of alpha-emitters with spectral analysis. Measuring with the "Normal" mode counts decays of both Polonium decay products of ^{222}Rn

(218Po, 214Po). The counts were measured over one hour and averaged, with a standard deviation of one sigma and expresses as decays per second [Bq]. The measurement range lies between $4 - 750000$ Bq m^{-3}

170 with an accuracy of ± 5 %.

The ^{222}Rn concentration in 300 mL water samples from ground water (2.3.3) and the river waswas measured with the Wat250 mode. In addition, soil ^{222}Rn emissions were estimated with closed chamber measurements with the RAD7 over 3h (one Rn measurement per hour). Assuming that groundwater is the main source of CO_2 and that ^{222}Rn moves at the same mass flow as CO_2 (Megonigal et al. 2020), the same

175 spatial dependence of CO_2 and ^{222}Rn fluxes would be expected in case of groundwater being the major source of CO_2. For this reason, ^{222}Rn chamber measurements were performed simultaneously at two different positions, one with low and one with high CO_2 flux. We used two chambers of different size and corrected ^{222}Rn flux measurements [Bq m^{-3} d^{-1}] for different chamber geometry by multiplying with the volume [m^3] and dividing by the area [m^2] of the chamber to get the ^{222}Rn flux [Bq m^{-2} d^{-1}].

180 **2.3.3 Water + sediment sampling**

For groundwater sampling piezometers with a diameter of 2.7 cm and a length of 100 cm were installed next to each collar (Figure S1b) a day before the sampling campaign.

To determine the thickness of the unsaturated zone, the water level in the piezometers was measured with an electric contact gauge. *In situ* parameters pH, conductivity, temperature, and O_2 saturation were

185 measured in the piezometers and the river with a multiparameter probe (WTW® MultiLine® Multi 3630 IDS, Xylem, Rye Brook, New York, USA). To analyze dissolved CO_2 and CH_4 concentrations, water samples were taken from the piezometers and the river using a syringe. Atmospheric air was added, with a headspace ratio of 1:1. After shaking for 2 minutes the headspace was transferred to 12 ml evacuated Exetainers (Labco Exetainers®, Labco Limited, Lampeter, UK) and stored till further analysis in the

190 laboratory. Air samples were taken for headspace correction. Water samples for chemical analysis were collected in crimp vials without a headspace, stored at 4 °C and later analyzed in the laboratory.

Soil samples from the 0-5 cm layer were taken around each collar for incubation experiments. Samples were filled into plastic bags, stored at 4°C, and were analysed in the laboratory within a week.

2.3.4 Potential CO₂ production in laboratory incubations of sediment

195 Incubation experiments were set up to analyze the potential microbial respiration in dry river sediments under controlled conditions. For this purpose, fresh soil samples (25 g wet weight), taken along the transect were incubated in ~ 130 ml vials in replicates of four at 19.5 °C. To determine the temperature dependence of microbial respiration, 4 replicate samples of 25 g were incubated at 4, 12, 19.5, 28 and 35 °C. From each vial, 4 to 5 gas samples were taken over an incubation period of 2 to 3 days by a Pressure-

200 Lok® syringe (Pressure-Lok® glass syringe, Valco Instruments, Waterbury, Houston, USA) and analyzed by gas chromatography for CO_2. Respiration rates were calculated from the linear increase of the CO_2 content in the incubation vials divided by dry sediment weight.

To evaluate the temperature response of the microbial respiration in the sediment the Q10 temperature coefficient and the activation energy (Ea) was calculated (Dell et al. 2011). The activation energy was

205 calculated as the slope of Arrhenius plots as described in Gillooly et al. (2001).

To compare respiration data from lab incubations to CO_2 fluxes measured in the field rates rates of respiration per gram dry weight [µmol g-dw d^{-1}] were converted to fluxes by multiplying with sediment bulk density [g-dw cm^{-3}] and the thickness of the reactive sediment layer which we assume to be equal to the thickness of the unsaturated zone [cm].

210 ## 2.4 Analytics

CO_2 and CH_4 concentrations in gas samples were measured with a gas chromatograph (GC) (SRI 8610C, SRI Instruments Europe, Bad Honnef, Germany). The GC was equipped with a flame ionization detector and a methanizer which allowed simultaneous measurement of CO_2 and CH_4 with an accuracy of < 5 %. Dissolved gas concentrations were calculated using temperature dependent Henry coefficients

215 (UNESCO/IHA 2010). Because the carbonate system in the headspace vial may change during headspace equilibration and CO_2 concentrations were corrected for alkalinity as described in Koschorreck et al. (2021).

To analyze dissolved inorganic carbon (DIC) and dissolved organic carbon (DOC) water samples were filtered with a glass microfiber filter (Whatman GF/F). DIC and DOC concentrations were analyzed based

220 on high-temperature oxidation and NDIR-Detection (DIMATOC® 2000, DIMATEC Analysentechnik,

Essen, Germany). The alkalinity of the water samples was determined by titration with HCl to pH of 4.3. To determine the concentration of the cations K^+, Na^+, Ca^{2+} and Mg^{2+} the water samples were filtered with a 0.45 µm syringe filter, acidified with HNO_3 and analyzed with an ICP OES (Optima 7300 DV, Perkin Elmer, USA). The Anion concentrations of SO_4^{2-} and Cl^- were measured with ion chromatography

225 (Dionex-ICS 6000, Thermo Fisher Scientific, Waltham, Massachusetts, USA).

Soil samples were analyzed to determine soil moisture content, bulk density, and organic matter from weight loss after ~~loss after~~ drying for at least 2 days to constant weight at 105 °C and loss on ignition (LOI) at 550°C, respectively. Sediment texture was determined by the FAO method (FAO 2020).~~To~~

~~analyze δ¹³C signatures of the organic matter, the sand and the organic matter in the sediment samples~~

230 ~~needed to be separated. This was done by suspending samples in ultrapure water followed by decanting~~ ~~and drying at 45 °C for 24 h. The dried and homogenized samples were analyses for carbon and nitrogen~~ ~~content and δ¹³C and δ¹⁵N signatures with an Element Analyzer connected to a mass spectrometer (EA~~ ~~IsoLink™ IRMS System, Thermo Fisher Scientific, Waltham, Massachusetts, USA).~~

2.5 Statistics

235 CO_2 flux data sets from manual and automatic measurements were visually checked for normality distribution with Q-Q-plots. ~~The CO_2 fluxes from the manual measurements were summarized by date~~ ~~and tested with univariate ANOVA and with the~~ with the post hoc Tukey's test~~paired t tests whether samples~~ ~~originate from the sample distribution and if groups differ significantly from each other. Additionally, the~~ ~~d~~Data were summarized by distance to the river and tested with a one-sample t-test to determine if

240 measured fluxes differed significantly from zero.

Spearman rank correlation was used to identify relationships between environmental variables and the observed CO_2 flux, and to identify the strength and direction of these relations (Leyer and Wesche 2007). Additionally, representative periods and single days were selected from automatic measurements to analyze patterns, hidden by the temporal variability of the data. The measured environmental variables of

245 sediment temperature, sediment moisture, thickness of the unsaturated zone, organic matter content, and precipitation were used for correlation analysis. Water level and climate data were averaged over 1 hour. Linear mixed-effects models (lme) were applied to predict the influence of the environmental variables

on the CO_2 flux at the study site for variables for which a linear relationship with the CO_2 flux was presumed. Model selection was done by removing predictors and comparing conditional R^2 values of

250 different models. To apply simple linear regression models and lme, assumptions of normality and homoscedasticity were visually checked with diagnostic plots, including residuals vs. fitted and Q-Q-plot. Flux data were log transformed for lme analysis. Because of occasional small negative fluxes we shifted all fluxes to positive values by adding 121 mmol m^{-2} d^{-1} prior to transformation (120 was is the value of the largest negative flux). Statistical analysis was performed using R (R-Core-Team 2016).

255 To evaluate the temperature response of the CO_2 flux as well as of microbial respiration in the sediment the Q10 temperature coefficient and the activation energy (Ea) was calculated . The activation energy was calculated as the slope of Arrhenius plots as described in Gillooly et al. (2001).

3 Results

3.1 Long term data

260 The river showed a typical summer discharge situation with a water level mostly below 1 m, interrupted by a high discharge event at the end of June (Figure 1). Considerable areas of dry sediments only emerged during 6 weeks in early summer, and short periods in the first week of August and in September. CO_2 fluxes measured during these periods showed high diurnal and seasonal fluctuations (Figure 2). Fluxes fluctuated over 3 orders of magnitude between -120 and 1135 mmol m^{-2} d^{-1} with a median of 98 and a

265 mean±SD of 149±155 mmol m^{-2} d^{-1}. Fluxes fluctuated in a narrow range below 200 mmol m^{-2} d^{-1} during the first phase of the investigations in May. Due to rising water level at May 17th we moved the chambers higher up where we measured both higher fluxes and larger diurnal amplitudes. When the water level decreased after May 20th we moved the chamber down to freshly emerged sediment. There, CO_2 fluxes were similar to the fluxes measured 10 cm higher during the first half of May and tended to increase with

270 increasing time since drying. Negative fluxes were observed in 193 out of 3128 flux measurements (=6% of all fluxes). Negative fluxes were observed especially during the beginning of the measurement period and at sites near to the water. Interestingly, negative fluxes nearly exclusively occurred during the day

between 10:00 and 18:00, peaking in the afternoon (Figure S2). Chambers installed closer to the water measured lower and less variable fluxes than chambers installed higher upslope.

275 Fluxes showed considerable short-term variability. Variability was not constant during the investigated period but especially high after June. Clear diurnal patterns were observed during the entire study but most pronounced in September.

280
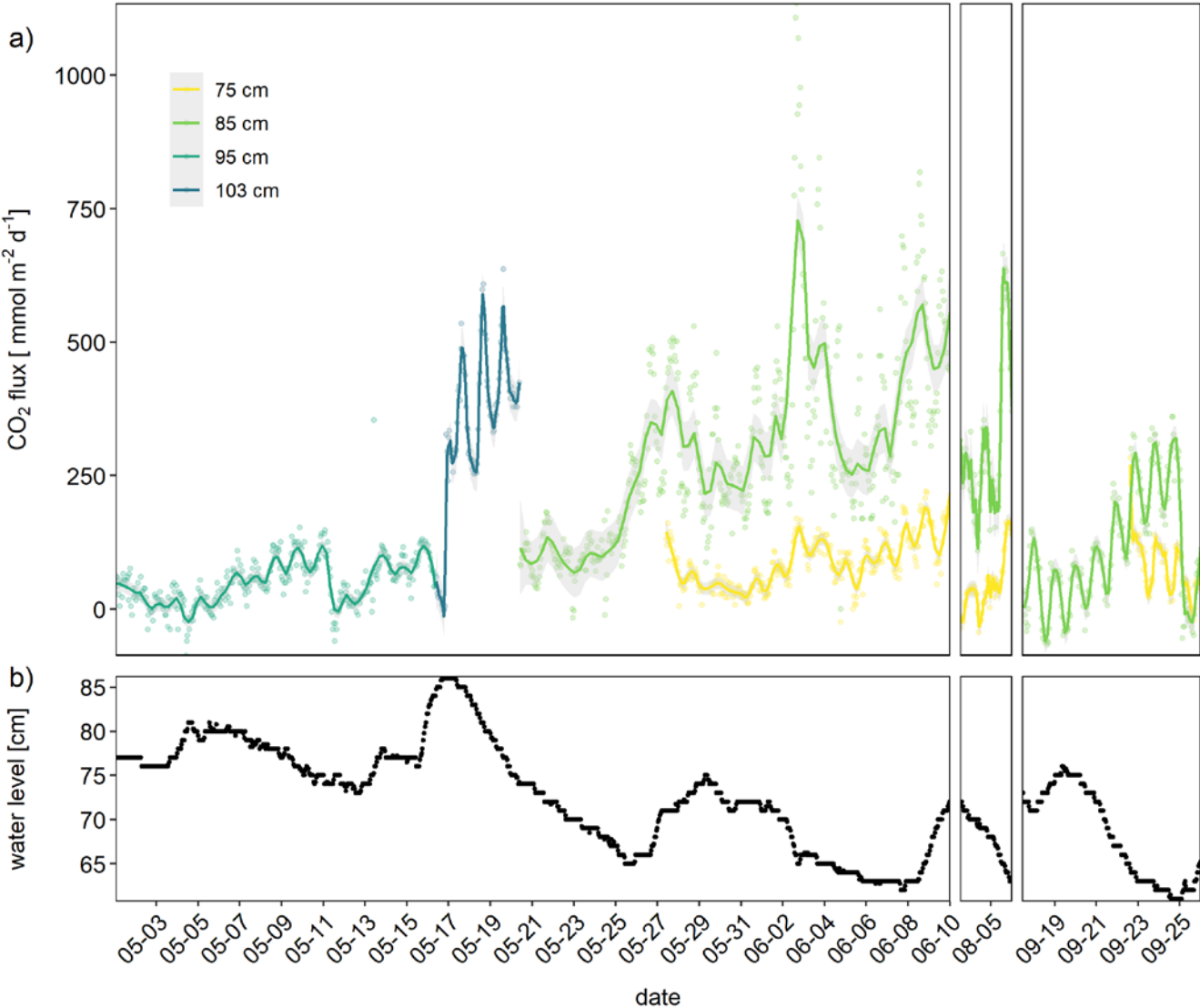
Figure 2: CO_2 fluxes in mmol m^{-2} d^{-1} measured with automatic chambers (a) and corresponding water level of the river measured 13 km downstream at the gauge "Magdeburg Strombrücke" (b). Colors indicate the position of the chamber relative to the gauge

(=elevation of the site), either 75, 85, 95, or 103 cm above current level. Lines indicate smoothed data ± SD using LOESS smoother with span 0.1~~the geom_smooth function in R (method="loess", span =0.1)~~. The grey areas indicate confidence intervals.

285 **3.1.1 Regulatory factors ~~HF~~: sediment moisture, temperature, water level, climate**

The observed diurnal pattern with higher CO_2 fluxes during the day suggested a temperature regulation of the flux. The CO_2 flux was indeed weakly (spearman $p<0.05$) correlated with the thickness of the unsaturated zone (R^2=0.31), sediment temperature (R^2=0.19, Figure 3a) and moisture (R^2=-0.19), as well as precipitation (R^2=-0.12). A mixed effect linear model with site were the chamber was placed as random

290 factor and temperature and thickness of the unsaturated zone as fixed factors explained 0.61 % of the variability. Adding moisture did not further improve the lme (Table S1).

The temperature response of the CO_2 flux was not very clear, however, if all data were plotted together (Figure 3a) but if data from single days were plotted a clear pattern emerged (Figure 3b and Figure S3). The temperature response of the flux was affected by the time of day resulting in typical hysteresis curves.

295 Warming during the day resulted in exponentially increasing fluxes. However, fluxes stayed high despite cooling started in the afternoon – the temperature response of the flux was clearly delayed. From the CO_2 flux-temperature relation (Figure 3a) an activation energy of 0.56 eV (37 kJ mol^{-1}) could be calculated which corresponds to a Q10 of 1.7 between 10 and 20°C.
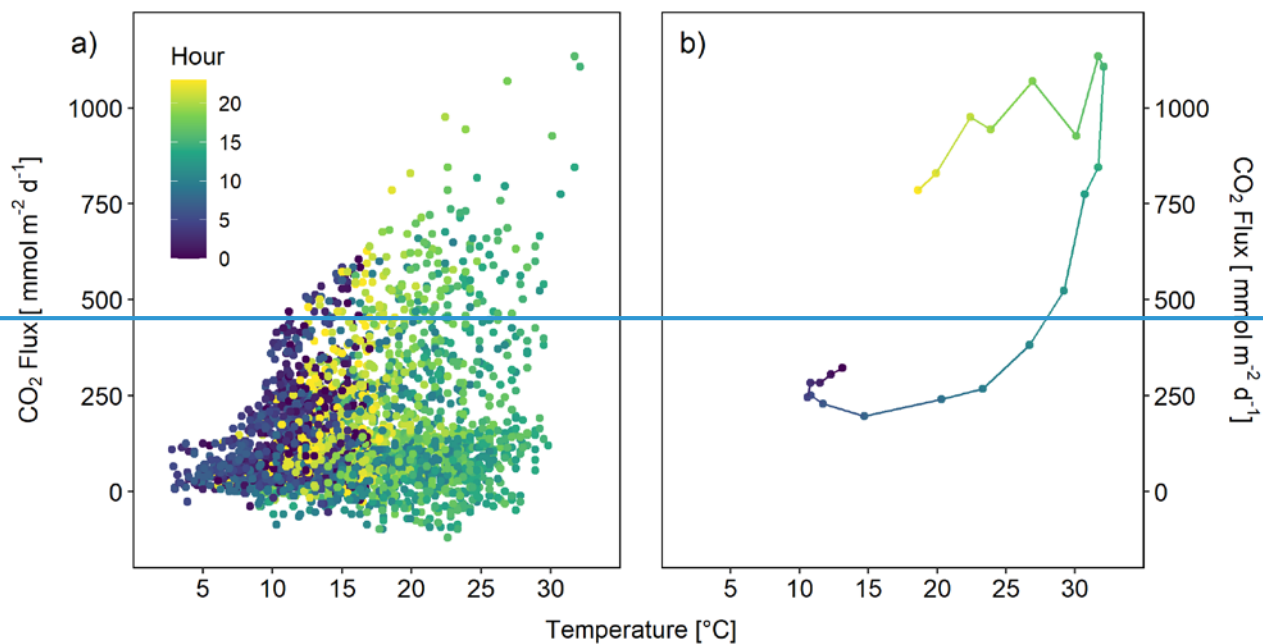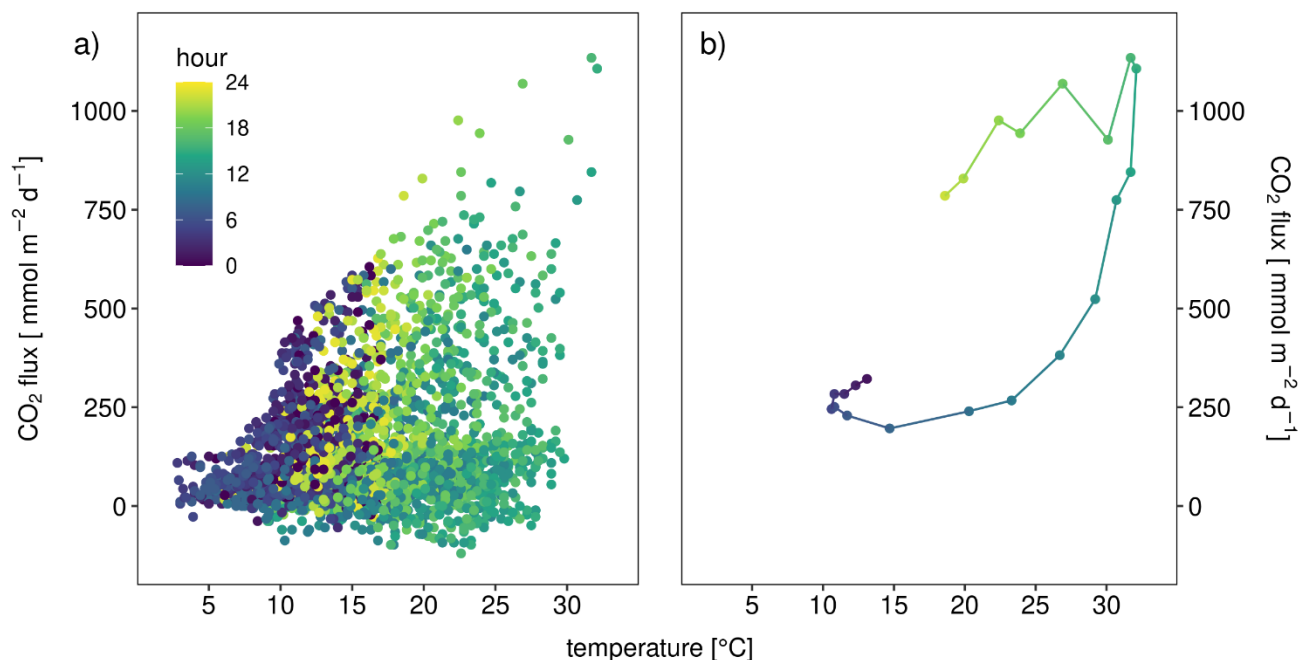
Figure 3: CO₂ flux in mmol m⁻² d⁻¹ (obtained from 3 automatic chambers) depending on sediment temperature (a) all data (b) only data from June 2ⁿᵈ as an example for hysteretic response to temperature. Color indicate hour of measurement.

A closer look at data from one week in September revealed how temperature, thickness of the unsaturated zone, and precipitation interacted in regulating the flux (Figure 4). Temperature drove the very clear

305 diurnal amplitude but the absolute level of the flux was higher with increasing thickness of the unsaturated zone (which was accompanied by sediment drying). A single precipitation event at September 25th resulted in a sudden increase in sediment moisture which was accompanied by a clear drop of the CO_2 flux. If only data for the period shown in Figure 4 were considered a linear model containing sediment temperature and moisture and the interaction between temperature and moisture explained 46 % of the

310 variance.
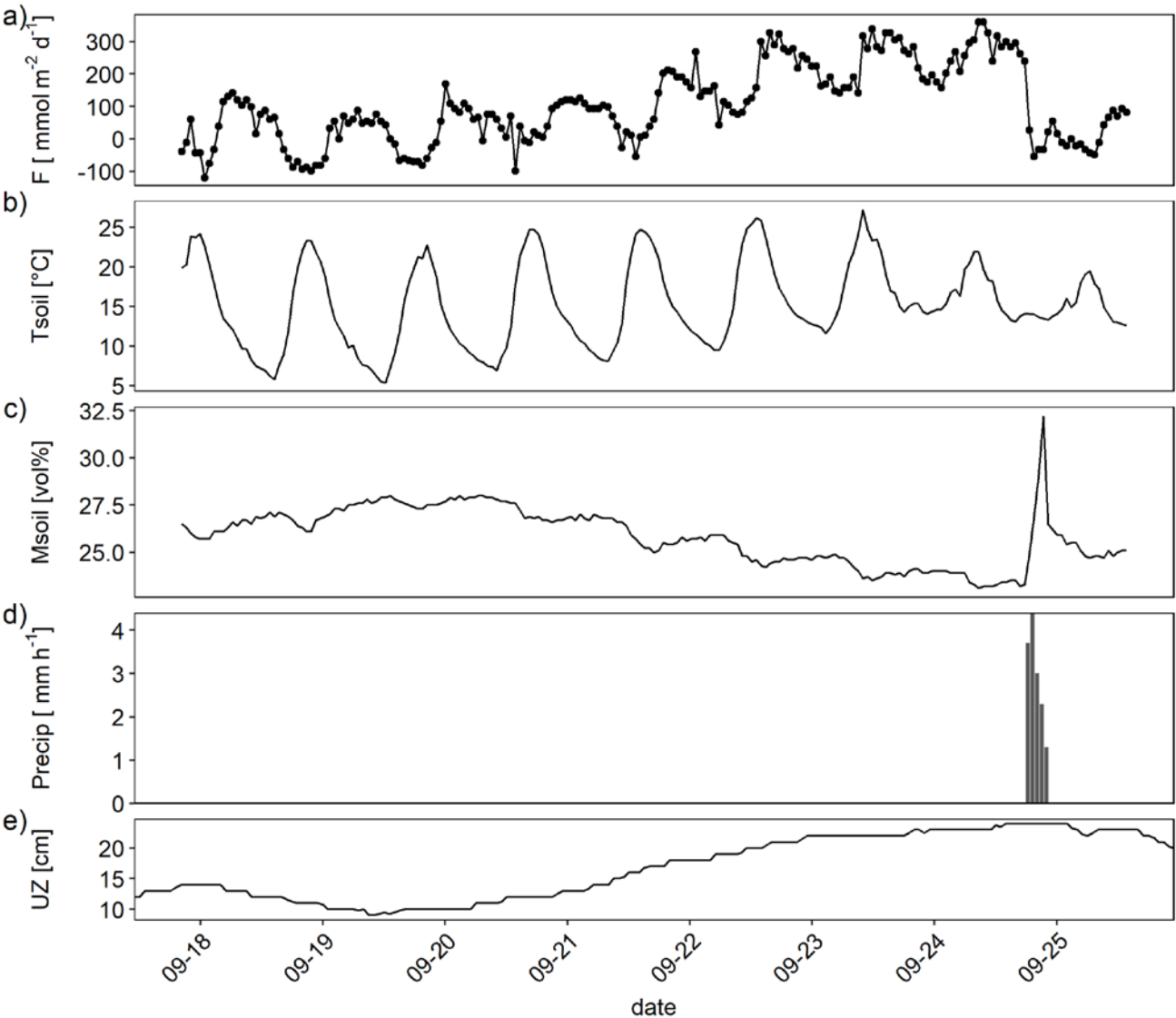
Figure 4: Example high frequency dataset showing (a) CO_2 flux (F) measured by an automatic chambers (b) sediment temperature (Tsoil; 0-5 cm depth) (c) sediment moisture (Msoil; 0-5 cm depth) (d) precipitation (Precip) recorded in hourly resolution and (e) thickness of the unsaturated zone (UZ; distance between water table level and ground surface).

3.1.2 Sspatial gradient of CO_2 flux

Manual As seen from the automatic chamber measurements at different distance to the water revealed, we observed a spatial gradient of the CO_2 flux. CO_2 fluxes were lowest near to the water line where sediment moisture was highest (Figure 5) and fluxes increased with distance to the water. This was also visible in the automatic chamber data when chambers were placed at different distance to the water (compare Figure 2). The chamber which was placed nearer to the water recorded consistently lower fluxes. This is also consistent with the observed positive correlation between CO_2 flux and the thickness of the unsaturated zone.
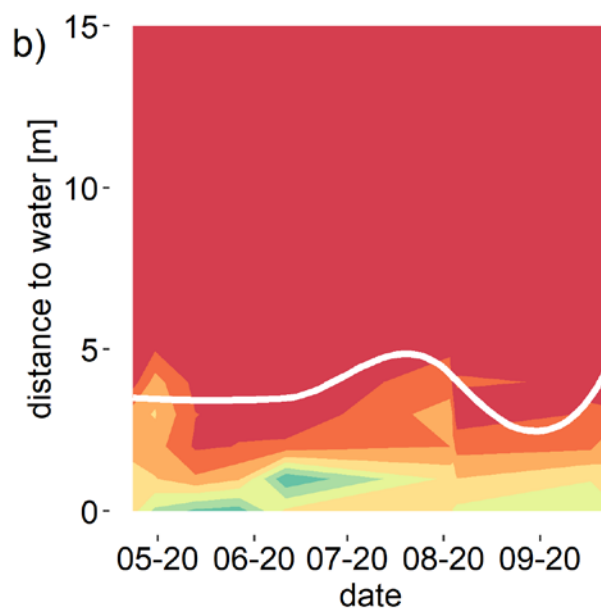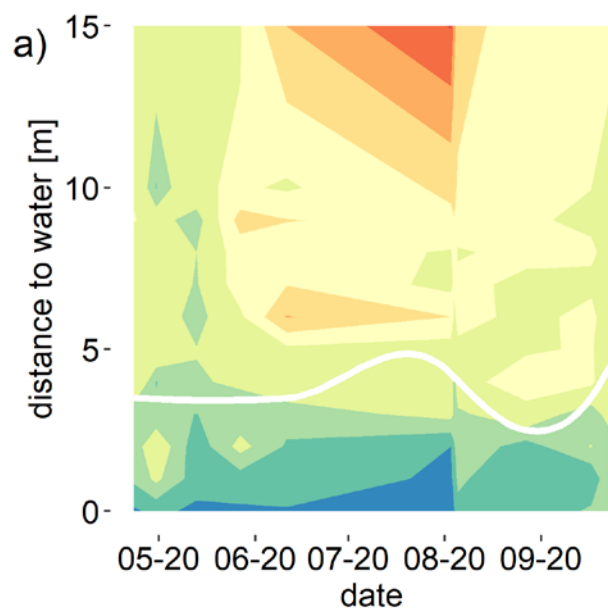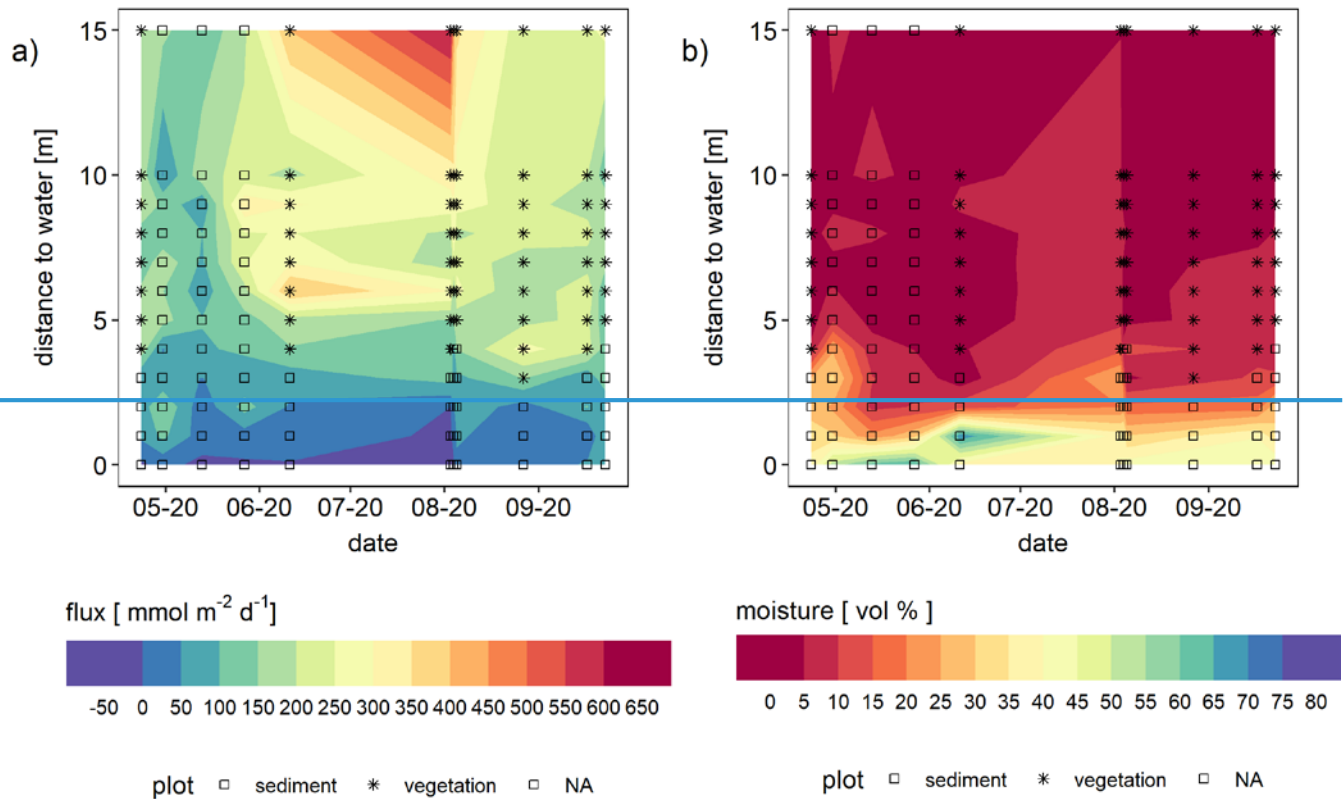
325 **Figure 5: CO_2 flux (mmol m^{-2} d^{-1}) as measured with a manual chamber (a) and sediment moisture (vol-%) measured with a probe in 0-5 cm depth (b) depending on the distance to the water. The white lines indicates the "plant line". The areas below this line was free of vegetation ~~Dots represent points of measurement and symbols indicate presence or absence of plants near to the chamber~~ (never plants inside chambers).**

We also observed higher CO_2 fluxes in the vicinity of plants. Plants were consistently found from about

330 3 m from the water uphill. Fluxes above this "plant line" (indicated by the white line~~symbols~~ in Figure 5)

tended to be higher than fluxes from the vegetation free area nearer to the water.

In sum, our field based measurements provide strong evidence that respiration in the sediment was the major driver of the observed CO_2 flux~~Taken this together there was strong evidence from field based flux measurements that respiration in the sediment was the major driver of the CO_2 flux~~. To further support

335 this conclusion detailed investigations were carried out.

3.2 Detailed investigations

The sediment pore water was quite similar to river water with respect to electric conductivity and dissolved solutes including DIC (Table 1). The water level difference between the wells and the river was below the detection limit – the hydraulic gradient was virtually zero during our sampling campaigns. The shallow hydraulic gradient and the similar chemistry suggest a large influence of river water on the sediment pore water. In contrast, concentrations of dissolved gases were quite different with high concentrations of CO_2 and CH_4, and low concentrations of O_2 in the pore water. Pore water concentrations of CO_2 increased with distance to the river while CH_4 concentrations tended to be highest near to the river. In August the river water was slightly under saturated with respect to CO_2. The sediment was poor in organic matter (LOI < 1%) and . Sediment texture as determined by the FAO method (FAO 2020) was loamy sand. GHG emissions were dominated by CO_2 while CH_4 fluxes were low and N_2O fluxes always below the detection limit (Table 1).

340

345

Table 1: Sediment, groundwater, and river water properties at the 2 sampling campaigns

parameter	unit	August 4th 20204.8.2020					September 23th 23.9.2020				
distance to river	m	river	1	3	5	6	river	1	2	3	4
CO_2 flux	mmol m^{-2} d^{-1}	-3	33	87	153	153	36	103	49	142	126
CH_4 flux	mmol m^{-2} d^{-1}	0.7	3.4	0	0	0.6	6	0.5	0	0	-0.6
unsaturated zone	cm		10	31	62	78		9	19	32	36.5
moisture	[vol %]		30	13	25	12		30	25	-	9
organic matter in sediment	[% LOI]		0.78	0.39	1.11	0.94		0.85	0.97	-	0.52
CH_4	µmol L^{-1}	0.3	18	11	11	6	2.5	189	186	212	70
CO_2	µmol L^{-1}	13.3	610	883	1960	3681	32	1193	899	1118	1024
DIC	mg L^{-1}	42	23	48	49	50	24	70	64	64	55

alkalinity	mg L^{-1}	1.9	3.5	3.5	3.6	3.1	1.9	4.5	4.8	5.3	4.7
DOC	mg L^{-1}	13.1	6.9	9.3	12	13.5	6.31	9.4	9.9	11.5	11
SO$_4^{2-}$	mg L^{-1}	79	44	71	67	74	79	7.3	20	31	92
pH		8.3	7.2	6.8	6.6	6.6	8	7.2	7.3	7.2	7
conductivity	µS cm^{-1}	640	610	658	640	1563	601	696	655	647	640
O$_2$	mg L^{-1}	9.1	0.8	1.1	1.9	2	9.3	3.4	2.5	4	4

Diffusive fluxes from the river were calculated from concentrations using the gas transfer coefficient from Matoušů et al. (2019).

3.2.1 CO$_2$ fluxes versus Rn fluxes

Groundwater contained more than one order of magnitude higher Rn concentrations than the river water (Table 2). As an indicator of groundwater evaporation and possible evasion of CO$_2$, we measured the flux of radon out of the sediment, assuming groundwater as a major source. Rn fluxes were higher in September than in August although the Rn concentration in the groundwater was similar in both months (Table 2). The flux of radon out of the sediment was, however, not much different at two different distances to the river while the CO$_2$ flux differed by about one order of magnitude between the same sites. If groundwater was the source of CO$_2$, we would expect Rn fluxes to be related to CO$_2$ evasion from groundwater; thus our data indicates that higher CO$_2$ fluxes were not driven by higher evaporation originating from groundwater.

Table 2: Flux of radon measured as ^{222}Rn increase in static chambers compared to CO$_2$ flux measured in the same chambers, and radon concentration determined as detected activity (Bq m^{-3}) in the groundwater sampled in wells directly beside the chambers as well as in the river water (0 m distance).

date	Distance to river [m]	^{222}Rn flux [Bq m^{-2} d^{-1}]	CO$_2$ flux [mmol m^{-2} d^{-1}]	^{222}Rn in GWwater [Bq m^{-3}]
5.8.202008-05	0			327±109
	1	65	18±20	6090±418
	3	63	110±31	
	0			532±135

09-	1	174	7±41	6650±436
23	4	205	169±36	

3.2.2 Sediment respiration rates

365 To check whether the observed CO_2 fluxes could be explained by microbial respiration in the sediment, laboratory incubations were carried out. Sediment respiration rates as measured in laboratory incubations were 0.9±0.45 µmol g^{-1} d^{-1} in August and 0.64 µmol g^{-1} d^{-1} in September with rates increasing with distance to the river. Potential CO_2 fluxes calculated from these rates were similar or higher than CO_2 fluxes measured *in situ* (Figure 6). Thus, sediment respiration was high enough to explain the observed

370 CO_2 emissions.
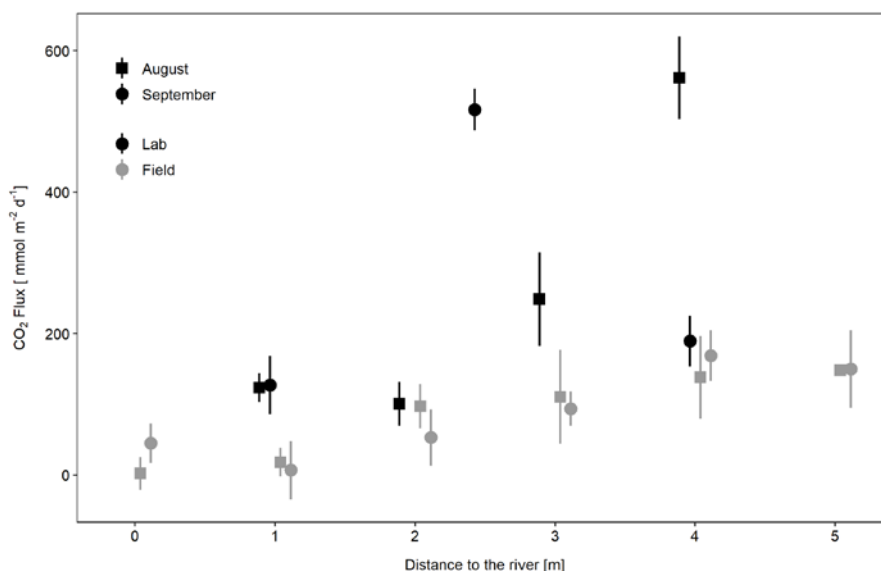
Figure 6: Potential CO_2 flux determined from laboratory incubations of sediment compared to *in situ* CO_2 fluxes depending on distance to the river. Potential fluxes per unit area were calculated from sediment respiration rates (mmol g^{-1} dw d^{-1}), the thickness of the unsaturated zone (cm), and the bulk density of the sediment (g dw cm^{-3}).

375 ### 3.2.3 Temperature dependence of sediment respiration

Sediment respiration increased exponentially with temperature (Figure 7) resulting in a Q10 of 2.5. The calculated activation energy of 0.7 eV was similar to the activation energy calculated from the automatic chamber data. The comparison with the temperature response of the CO_2 flux measured by the automatic

chambers (line in Figure 7) visualizes the similar temperature response of sediment respiration and *in situ*

380 fluxes.
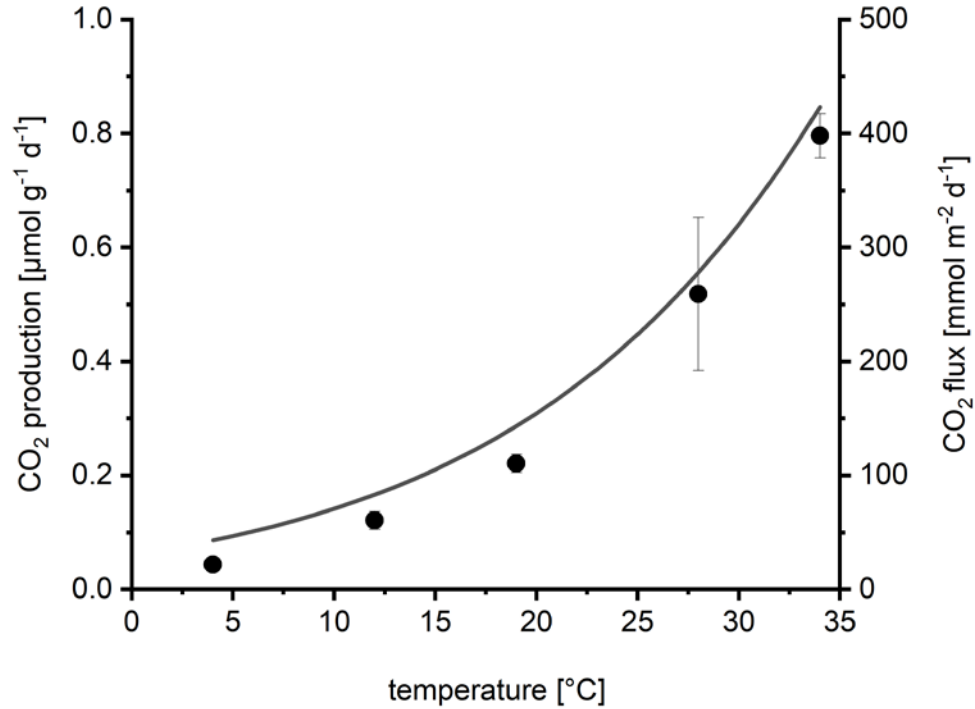
Figure 7: Temperature dependence of Sediment CO₂ production (=sediment respiration) in laboratory incubations depending on temperature (dots show mean±SD of 4 replicates). For comparison, the line shows the average temperature response of the CO₂ flux measured by automatic chambers, calculated by fitting the data from Figure 3a to the Arrhenius equation.

385 # 4 Discussion

4.1 Source of the CO₂

Both our continuous data and detailed measurements show that the CO_2 emitted from dry Elbe sediments originated from respiration in the sediment rather than ~~from~~ groundwater ~~evasion~~. This conclusion is consistently supported by numerous evidence:

390 • The observed CO_2 fluxes could be fully explained by sediment respiration measured in laboratory incubations. From soil respiration measurements it is well known that basal respiration as measured in laboratory incubations cannot be equaled with soil CO_2 emissions (Reichstein et al.

2000). A major difference between both methods is the exclusion of root respiration in bottle incubations which would lead to an under estimation of total soil respiration in root free assays such as bottle incubations (Hanson et al. 2000). Thus, our sediment respiration rates measured in the laboratory are probably conservative estimates which even strengthens our argumentation.

- The temperature response of the CO_2 flux was very similar to the measured temperature response of sediment respiration and showed Q10 values typical for biological processes (Yvon-Durocher et al. 2012) and soil respiration (Hamdi et al. 2013). Potential evaporation on the other hand depends on radiation, vapor pressure, and wind speed (Penman 1948) and only indirectly on surface temperature (Kidron and Kronenfeld 2016). The temperature dependence of evaporation of soils depends on a complex interaction of texture and soil moisture, and is not easy to predict (e.g. (Federer 2002)). The observed temperature dependence provides strong evidence for respiration being the primary driver of the CO_2 flux.

- CO_2 emissions increased with distance to the river. If groundwater evasion was a major source of CO_2 emissions we would expect higher emissions at lower sediment elevation were groundwater potentially exfiltrates into the sediment. If there was a hydraulic groundwater gradient towards the river this gradient should be steepest near to the river resulting in highest groundwater flux and potential outgassing near the river.

- The CO_2 flux was proportional to the volume of the unsaturated sediment. If CO_2 originated from groundwater emissions we would expect even a negative correlation because the transport of CO_2 from the groundwater surface to the sediment surface should be inhibited by a larger unsaturated zone.

- Higher CO_2 emissions were not accompanied by higher Rn emissions. Groundwater typically contains high Rn concentrations and Rn is a proven tracer to investigate groundwater input into surface waters (Cook and Herczeg 2000; Perkins et al. 2015). We observed emission of Rn from the sediments indicating some influence of groundwater on the sediments. Rn emission at different distance from the river were identical. Thus, the thickness of the unsaturated sediment did not affect Rn emissions, showing that the anoxic zone itself was probably not a source of Rn. Soil Rn concentrations are known to be affected by meteorological and soil physical conditions (Asher-

Bolinder et al. 1971). Similar Rn emissions, as observed in our study, are therefore an indication for similar sediment physical conditions. However, the magnitude of Rn emissions did not correspond to the magnitude of the CO_2 emissions, indicating that the CO_2 flux was independent from groundwater outgassing.

425   • As we did not see hydraulic gradients indicative of larger groundwater inflow at our location of study, unrealistic high evaporation rates would be necessary to explain the observed CO_2 flux with groundwater evasion. Groundwater degassing is relevant in situation when groundwater is pumped to the surface (Wood and Hyndman 2017) or seeps into surface waters (Duvert et al. 2018). In rivers it might be relevant at seep sites which probably especially occur after fast water
430   level drops and at extremely low water level.

Taken together our data consistently show that the observed CO_2 emissions originated from respiratory CO_2 production in the sediment. After having identified the primary source of CO_2 we now look on the regulators of the magnitude of the CO_2 emissions.

4.2 Regulation of CO_2 emissions

435   Temperature is a master variable regulating several biogeochemical processes. Our temperature dependence (Q10 = 2.5, Ea 0.7 eV) is in line with the temperature response of numerous ecological processes. A meta analysis of 63 studies of temperature dependence of soil respiration revealed a mean Q10 of 2.6 (Hamdi et al. 2013). Diverse types of ecosystems have an activation energy of respiration of 0.65 eV (Yvon-Durocher et al. 2012) which is very similar to our study.

440   Temperature was an important regulator not only because of the temperature dependence of sediment respiration but also because the diurnal temperature amplitude was quite large. Sediment temperature not only ranged between 2.8 and 32°C during the study period but the complete temperature amplitude of about 20°C could be observed during single days (Figure 4). The large diurnal amplitude at these sites is favored by a lack of shadow and the fast heating of the sand which can lead to temperatures easily
445   exceeding 40°C (Mallast et al. 2020).

Although the temperature dependence of the CO_2 flux is evident, it was not easily visible in flux versus temperature plots which show a large scatter (Figure 3a). Only when looking at single days a typical

hysteresis pattern (Figure 3b) became apparent. Such hysteresis curves have frequently been observed in high frequency datasets of soil respiration (e.g. (Riveros-Iregui et al. 2007)). They originate from a phase lag between temperature and CO_2 flux and can be explained by different transport of heat and CO_2 in soils (Phillips et al. 2011) or by variable C supply from plants (Oikawa et al. 2014). The rotation direction as well as the shape of the ellipsoid depends on the vertical profile of temperature and activity in the soils as well as on the depth were soil temperature was measured. We measured temperature in 5 cm depth and obtained anticlockwise hysteresis which means that CO_2 emissions were delayed relative to temperature measurements. A plausible explanation is that a large part of the CO_2 was produced in deeper sediment layers where the daily temperature maximum was reached later. This is consistent with the observed positive correlation between CO_2 flux and the thickness of the unsaturated zone. Theoretically the effect could also be caused by delayed outgassing of CO_2 from deeper sediment layers due to CO_2 transport limitation. However model calculations had shown that this mechanism was less relevant for shaping diurnal hysteresis in soils (Phillips et al. 2011). We quantified the delay by shifting flux and sediment-temperature data against each other (Figure 8Figure S3). By correlating the flux with the temperature 3 hours before we obtained the best linear correlation (R^2=0.97) for the data in Figure 3b). However, the time shift which produced the best linear fit differed between days (min=0, max=10, mean±SD = 4.8±3.7 h) with a median of 4 hours and no apparent differences between sites. Also the R^2 of the best fit differed between 0.2 and 0.97. Thus, the hysteresis pattern obviously depended on the day of measurement and it is not possible to derive a general relation which then could be used to analyze temperature-flux relations of time-shift corrected data.
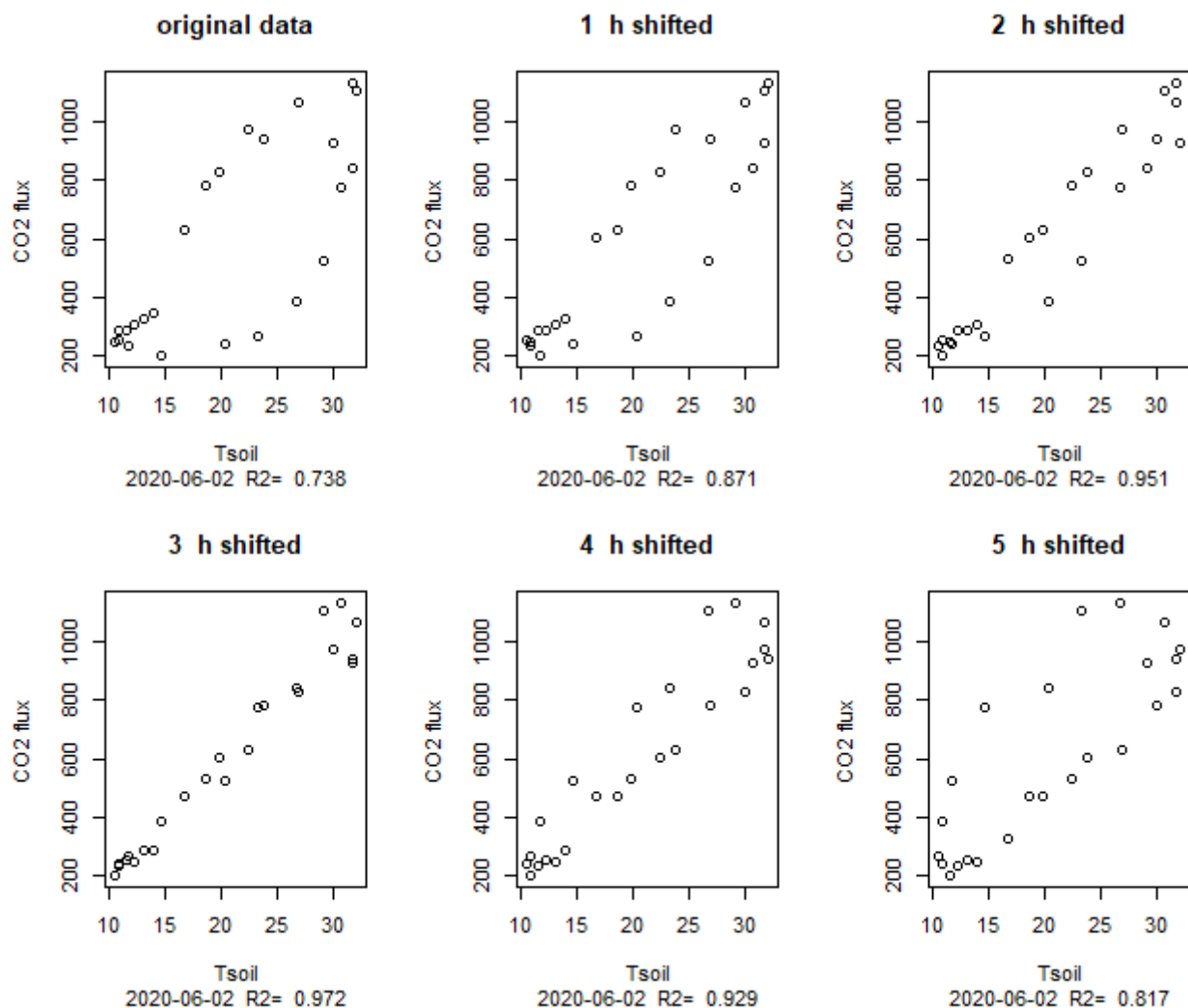
Figure 8: Hysteresis loop for June 2nd (same data as in Figure 3b) with flux data shifted for various hours. 3 hours shifted means that the flux at 10:00 was correlated with the temperature at 7:00.

Wetting of dry soils typically triggers a pulse of CO_2 production (Birch 1958). However, in our case wetting events caused by rainfall reduced the CO_2 flux as exemplified in Figure 4. This shows that CO_2 production in the sediment was not water limited and/or that the CO_2 flux was rather transport limited when rain water blocked gas filled pores (Asher-Bolinder et al. 1971). At sediment moisture around 30% in sandy sediments as measured in our study microbial activity in the sediment is probably not water

stressed and consequently not stimulated by wetting. Thus, it is probable that the reduced CO_2 flux after rain events was caused by physical blocking of soil pores. This is consistent with the observed long term

480 increase of the CO_2 flux with decreasing moisture. Direct mechanistic dependence, however, is difficult to show because moisture also correlates with the thickness of the unsaturated zone (=water level of the river relative to the sediment surface). This is why adding moisture to our mixed model only marginally increased the predictive power of the statistical model.

The thickness of the unsaturated zone was a strong predictor of the CO_2 flux. The entire unsaturated zone

485 obviously contributed to the CO_2 flux. This is plausible because the intermediate sediment moisture both favored microbial processes and enabled gas exchange through gas filled pores. This may also explain high CO_2 fluxes in situations with extremely high sediment surface temperature (Mallast et al. 2020). Even if under such conditions CO_2 production is inhibited at the surface respiration in deeper layers may maintain high CO_2 emissions.

490 The occurrence of vegetation, although excluded from our chamber measurements and restricted to the vicinity of the chambers, obviously is a game-changer, largely stimulating sediment CO_2 emissions. From our data we cannot fully distinguish whether higher fluxes near plants were caused by the plants or only by distance to the water (which is equivalent to the thickness of the unsaturated zone). However, the thickness of the unsaturated zone increased continuously while the "plant line" represents a sudden

495 change of conditions. Our data show a consistent high CO_2 flux above the "plant line". It is well known that root respiration may contribute about 50% to soil respiration (Hanson et al. 2000) and soil respiration is typically correlated with root biomass (Tufekcioglu et al. 2001). Thus, as we did not use trenched collars to exclude roots from chamber fluxes, it is highly probable that plants contributed to the elevated CO_2 emissions through root respiration or provision of root exudates above the "plant line". Higher sediment

500 CO_2 emissions, however, do not mean net CO_2 emissions from the ecosystem since the vegetation growing on the dry sediments also fixes carbon and can even turn exposed sediments into a carbon sink (Bolpagni et al. 2017). To assess the effect of emerging vegetation on the overall carbon cycle of dry sediments other methods like plant biomass determination or flux measurements including photosynthesis in transparent chambers are necessary.

4.3 CO₂ uptake by the sediment

We frequently observed CO_2 uptake by the sediment, although there were no plants and no light in our chamber. This is know from other studies and has been attributed to inorganic processes (Ma et al. 2013; Marcé et al. 2019). In our case the observed CO_2 uptake could also be explained by the interaction of the sediment with river water. During May and June the river was under saturated with CO_2 (Fig. Figure S4). The groundwater chemistry data show a gradient of concentrations increasing with distance to the river. This shows that the sediment pore water near to the river was affected by river water. Interestingly, negative fluxes were nearly exclusively observed during the daylight hours. A plausible explanation would be that ship induced wave action might have triggered occasional river water intrusion and CO_2 uptake by the sediment (Hofmann et al. 2010). This mechanism, however, cannot explain negative fluxes in September when the river was over saturated with CO_2 (Fig. Figure S4).

Dark CO_2 uptake could theoretically be caused by chemoautotrophic micro-organisms like nitrifiers. However, chemoautotrophic CO_2 uptake should not be stimulated by light and is thus not consistent with our observation of nearly exclusive CO_2 uptake during the day.

A straightforward explanation for negative CO_2 fluxes during the day is CO_2 uptake by phototrophic organisms. Algae and cyanobacteria are well known to have active carbon concentrating mechanisms (CCM) which allow CO_2 uptake also in the dark (Giordano et al. 2005). Phototrophs living at the surface of dry sediments are facing a harsh environment with high salinity in thin water films covering particles and high irradiation and temperature – all factors favoring the activation of CCMs (Beardall and Giordano 2002). Dark CO_2 uptake is a common observation in $^{14}CO_2$ uptake measurements and known to depend on pre-darkness light conditions (Legendre et al. 1983). In pure cultures it has been shown that CO_2 uptake by algae may proceed for more than an hour in darkness (Goldman and Dennett 1986; Ohmori et al. 1984). Thus, it is highly plausible that the observed CO_2 uptake by dry sediments was caused by photosynthetic algae and/or cyanobacteria. Future studies including chlorophyll analysis of sediments or the application of specific inhibitors may clarify the mechanism behind CO_2 uptake in exposed river sediments.

4.4 Implications

Photosynthetic uptake of CO_2 in the dark would have consequences for the interpretation of dark chamber measurements. If a chamber is placed on the sediment photosynthetic CO_2 uptake may proceed for an unknown period of time. The fact that no net uptake was observed in the night shows that the capability of dark CO_2 uptake could not be sustained for periods longer than one hour, which is consistent with pure culture observations (Goldman and Dennett 1986). However, flux measurements are usually performed within a few minutes making it highly probable that they include eventual photosynthetic CO_2 uptake. Comparison of transparent and opaque chamber measurements are sometimes used to detect photosynthesis of algae. Our results imply that such interpretation have to be treated with care because photosynthetic CO_2 uptake may proceed during dark flux measurements.

Our median CO_2 flux of 98 mmol m^{-2} d^{-1} would result in annual emissions of 429 g C m^{-2} y^{-1} which is in the range of fluxes typical for temperate ecosystems (Doering et al. 2011) and similar to fluxes reported for dry Elbe sediments (Mallast et al. 2020), but high compared to the gravel bed of an alpine river (38 mmol m^{-2} d^{-1}, (Doering et al. 2011)), and low compared to exposed sediments of Mediterranean streams (781 mmol m^{-2} d^{-1}, Gómez-Gener et al. (2016)). Although our observations thus fit the reported range, these differences as well as the large variation of fluxes observed in our high frequency measurements (-120 to 1135 mmol m^{-2} d^{-1} – this range is larger than the range of typical fluxes for all kinds of terrestrial ecosystems as compiled by (Doering et al. 2011)) implies that care must be taken when upscaling fluxes for certain ecosystems but also for larger scales.

The observed hysteresis obscures flux-temperature relations if measurements were only performed at one time during the day. Thus, temperature regulation of dry sediment CO_2 emissions might be more relevant and more complex than identified in a recent study (Keller et al. 2020).

Our high frequency measurements show that standard measuring protocols are probably under estimating CO_2 emissions from dry sediments because high fluxes in the night resulting from a delayed temperature response are not considered. The median flux measured between normal working hours (8:00 – 18:00) was 87 mmol m^{-2} d^{-1} compared to 98 mmol m^2 d^{-1} if all data were considered. Thus, only measuring during daytime would lead to a flux under estimation of 11%. We therefore recommend to assess temporal

shifts in flux-temperature responses in order to obtain better estimates for upscaling based on a representative choice of flux data.

560 Our results are partly contradicting results from (Mallast et al. 2020) who observed highest CO_2 emissions near to the waterline. The two studies, however, are not directly comparable because the previous study by (Mallast et al. 2020) was carried out under extreme drought conditions. Under such conditions deeper lying sediments which tend to be higher in organic matter and less sandy were exposed to the atmosphere. Such conditions should favor CO_2 emissions (Keller et al. 2020). Furthermore the very dry conditions

565 (<10% sediment moisture) under the extreme drought might have inhibited microbial processes in the sandy sediment. While the drivers of CO_2 emissions from dry sediments are known, their complex interaction makes it difficult to predict CO_2 emissions under a given situation.

The observed relation between CO_2 flux and distance to the river, however, might facilitate upscaling of CO_2 emissions from dry river sediments. The width of the dry sediment zone can be extracted from

570 satellite images or aerial photographs. The observed consistent spatial pattern also implies that the CO_2 flux was probably not much affected by time after exposure. Thus, combining few diurnal datasets of CO_2 flux and lateral transects with seasonal data of the width of the dry sediments zone along a river is a promising approach to quantify total CO_2 emissions from such systems.

5 Conclusions

575 We could clearly show that CO_2 emissions from dry river sediments under the given conditions here were primarily driven by respiration in the sediment. Thus, existing knowledge about soil respiration might also apply to dry river sediments.

We could further show that CO_2 emissions were regulated by temperature and the thickness of the unsaturated zone (Figure 8). The observed hysteresis effect clearly show that simple correlations between

580 environmental parameters and CO_2 emissions from sediments may be too simplistic to study regulatory mechanisms. Positively spoken the analysis of such hysteresis relations may allow conclusions about underlying mechanisms (Musolff et al. 2021).
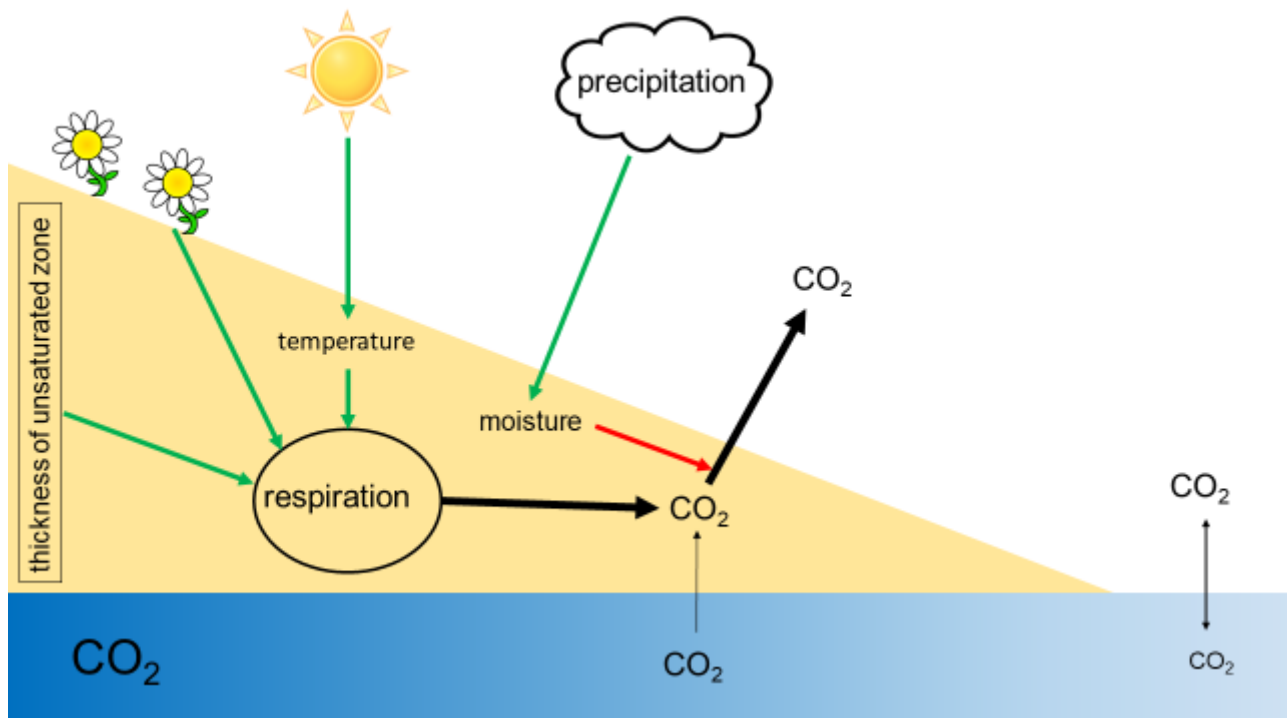
Figure 9: Scheme of processes and drivers of CO_2 fluxes from dry river sediments. Green arrows indicate positive, red arrows negative effects.

Our data show that the occurrence of terrestrial vegetation has a large and not yet assessed impact on the carbon cycle of dry sediments. To assess the effect of vegetation not only ecosystem production has to be quantified but also the fate of plant biomass upon re-flooding. While it is clear that CO_2 emissions from dry river sediments are relevant the exact quantification of the effect of low river levels on the river carbon cycle remains challenging. Short term temporal ~~dynamics~~ variation is very high and probably equally relevant as seasonal variability. Any attempt to quantify annual GHG emissions or the relevance of dry river sediments for carbon cycling needs to address temporal dynamics of CO_2 emissions from dry river sediments.

6 Data availability

The high frequency dataset is supplied as a supplement.

7 Supplement link

8 Author contribution:

MK initiated the study and prepared the manuscript with contributions from all co-authors. LT and MK performed measurements. All authors planned measurements and discussed the results.

9 Competing interests

The authors declare that they have no conflict of interest.

10 Acknowledgements

Thanks to Martin Wieprecht for his excellent help during fieldwork and to Ulrike Berning-Mader and Corinna Völkner for their instructions and help in the laboratory of the Westfälische Wilhelms-University and UFZ. Thanks to Prof. Christian Wilhelm for advice regarding dark CO_2 fixation and to Peifang Leng for help using R. This work was supported by funding from the Helmholtz Association in the framework of Modular Observation Solutions for Earth Systems (MOSES).

11 References

Asher-Bolinder, S., D. E. Owen, and R. R. Schumann. 1971. A PRELIMINARY EVALUATION OF ENVIRONMENTAL FACTORS INFLUENCING DAY-TO-DAY AND SEASONAL SOIL-GAS RADON CONCENTRATIONS. *In* L. C. S. Gundersen and R. B. Wanty [eds.], Field Studies of radon in rocks, soils, and water. U.S: Geological Survey.

Battin, T. J., S. Luyssaert, L. A. Kaplan, A. K. Aufdenkampe, A. Richter, and L. J. Tranvik. 2009. The boundless carbon cycle. Nature Geoscience **2:** 598-600.

Beardall, J., and M. Giordano. 2002. Ecological implications of microalgal and cyanobacterial CO_2 concentrating mechanisms, and their regulation. Funct. Plant Biol. **29:** 335-347.

Birch, H. F. 1958. The effect of soil drying on humus decomposition and nitrogen availability. Plant Soil **10:** 9-31.

Bolpagni, R., S. Folegot, A. Laini, and M. Bartoli. 2017. Role of ephemeral vegetation of emerging river bottoms in modulating CO_2 exchanges across a temperate large lowland river stretch. Aquat. Sci. **79:** 149-158.

Bolpagni, R., A. Laini, T. Mutti, P. Viaroli, and M. Bartoli. 2019. Connectivity and habitat typology drive CO_2 and CH_4 fluxes across land–water interfaces in lowland rivers. Ecohydrology **12:** e2036.

Bussmann, I., U. Koedel, C. Schütze, N. Kamjunke, and M. Koschorreck. 2022. Spatial Variability and Hotspots of Methane Concentrations in a Large Temperate River. Front Env Sci-Switz **10**.

Cook, P. G., and A. L. Herczeg. 2000. Environmental Tracers in Subsurface Hydrology. Springer.

Coppola, E., M. Verdecchia, F. Giorgi, V. Colaiuda, B. Tomassetti, and A. Lombardi. 2014. Changing hydrological conditions in the Po basin under global warming. Sci Total Environ **493:** 1183-1196.

Dell, A. I., S. Pawar, and V. M. Savage. 2011. Systematic variation in the temperature dependence of physiological and ecological traits. P Natl Acad Sci USA **108:** 10591-10596.

Doering, M., U. Uehlinger, T. Ackermann, M. Woodtli, and K. Tockner. 2011. Spatiotemporal heterogeneity of soil and sediment respiration in a river-floodplain mosaic (Tagliamento, NE Italy). Freshwat. Biol. **56:** 1297-1311.

Duvert, C., D. E. Butman, A. Marx, O. Ribolzi, and L. B. Hutley. 2018. CO_2 evasion along streams driven by groundwater inputs and geomorphic controls. Nature Geoscience **11:** 813-818.

DWD. 2020. Datenbasis. Einzelwerte gemittelt. *In* D. Wetterdienst [ed.]. German Weather Service.

FAO. 2020. Soil testing methods: global soil doctors programme-a farmer to farmer training programme., Soil testing methods manual.

Federer, C. A. 2002. BROOK 90: A simulation model for evaporation, soil water, and streamflow.

Gillooly, J. F., J. H. Brown, G. B. West, V. M. Savage, and E. L. Charnov. 2001. Effects of size and temperature on metabolic rate. Science **293:** 2248-2251.

Giordano, M., J. Beardall, and J. A. Raven. 2005. CO_2 concentrating mechanisms in algae: Mechanisms, environmental modulation, and evolution. Annu. Rev. Plant Biol. **56:** 99-131.

Goldman, J. C., and M. R. Dennett. 1986. Dark CO_2 Uptake by the Diatom Chaetoceros-Simples in Response to Nitrogen Pulsing. Mar. Biol. **90:** 493-500.

Gómez-Gener, L. and others 2016. When Water Vanishes: Magnitude and Regulation of Carbon Dioxide Emissions from Dry Temporary Streams. Ecosystems **19:** 710-723.

Gomez-Gener, L. and others 2015. Hot spots for carbon emissions from Mediterranean fluvial networks during summer drought. Biogeochemistry **125:** 409-426.

Hamdi, S., F. Moyano, S. Sall, M. Bernoux, and T. Chevallier. 2013. Synthesis analysis of the temperature sensitivity of soil respiration from laboratory studies in relation to incubation methods and soil conditions. Soil Biology & Biochemistry **58:** 115-126.

Hanson, P. J., N. T. Edwards, C. T. Garten, and J. A. Andrews. 2000. Separating root and soil microbial contributions to soil respiration: A review of methods and observations. Biogeochemistry **48:** 115-146.

Hofmann, H., L. Federwisch, and F. Peeters. 2010. Wave-induced release of methane: Littoral zones as a source of methane in lakes. Limnol. Oceanogr. **55:** 1990-2000.

Keller, P. S. 2020. glimmr: Compute gasfluxes with R. Gas Fluxes and Dynamic Chamber Measurements.

Keller, P. S. and others 2020. Global CO_2 emissions from dry inland waters share common drivers across ecosystems. Nature Communications **11:** art. 2126.

Kidron, G. J., and R. Kronenfeld. 2016. Temperature rise severely affects pan and soil evaporation in the Negev Desert. Ecohydrology **9:** 1130-1138.

Koschorreck, M., Y. T. Prairie, J. Kim, and R. Marce. 2021. Technical note: CO_2 is not like CH_4 - limits of and corrections to the headspace method to analyse pCO_2 in fresh water. Biogeosciences **18:** 1619-1627.

Legendre, L., S. Demers, C. M. Yentsch, and C. S. Yentsch. 1983. The C-14 Method - Patterns of Dark CO_2 Fixation and DCMU Correction to Replace the Dark Bottle. Limnol. Oceanogr. **28:** 996-1003.

Leyer, I., and K. Wesche. 2007. Multivariate Statistik in der Ökologie. Eine Einführung. Springer.

Ma, J., Z.-Y. Wang, B. A. Stevenson, X.-J. Zheng, and Y. Li. 2013. An inorganic CO_2 diffusion and dissolution process explains negative CO_2 fluxes in saline/alkaline soils. Sci Rep-Uk **3:** 2025.

Machado dos Santos Pinto, R., G. Weigelhofer, E. Diaz-Pines, A. Guerreiro Brito, S. Zechmeister-Boltenstern, and T. Hein. 2020. River-floodplain restoration and hydrological effects on GHG emissions: Biogeochemical dynamics in the parafluvial zone. Sci Total Environ **715:** 136980.

Macpherson, G. L. 2009. CO_2 distribution in groundwater and the impact of groundwater extraction on the global C cycle. Chemical Geology **264:** 328-336.

Mallast, U., M. Staniek, and M. Koschorreck. 2020. Spatial upscaling of CO_2 emissions from exposed river sediments of the Elbe River during an extreme drought. Ecohydrology **13**.

Marcé, R. and others 2019. Emissions from dry inland waters are a blind spot in the global carbon cycle. Earth-Sci. Rev. **188:** 240-248.

Martinsen, K. T., T. Kragh, and K. Sand-Jensen. 2019. Carbon dioxide fluxes of air-exposed sediments and desiccating ponds. Biogeochemistry.

Matoušů, A., M. Rulík, M. Tušer, A. Bednařík, K. Šimek, and I. Bussmann. 2019. Methane dynamics in a large river: a case study of the Elbe River. Aquat. Sci. **81:** 12.

Musolff, A. and others 2021. Spatial and Temporal Variability in Concentration-Discharge Relationships at the Event Scale. Water Resources Research **57:** e2020WR029442.

Ohmori, M., S. Miyachi, K. Okabe, and S. Miyachi. 1984. Effects of Ammonia on Respiration, Adenylate Levels, Amino-Acid Synthesis and Co2 Fixation in Cells of Chlorella-Vulgaris 11h in Darkness. Plant and Cell Physiology **25:** 749-756.

Oikawa, P. Y., D. A. Grantz, A. Chatterjee, J. E. Eberwein, L. A. Allsman, and G. D. Jenerette. 2014. Unifying soil respiration pulses, inhibition, and temperature hysteresis through dynamics of labile soil carbon and O2. Journal of Geophysical Research: Biogeosciences **119:** 521-536.

Palmia, B., S. Leonardi, P. Viaroli, and M. Bartoli. 2021. Regulation of CO_2 fluxes along gradients of water saturation in irrigation canal sediments. Aquat. Sci. **83:** 18.

Penman, H. L. 1948. Natural Evaporation from Open Water, Bare Soil and Grass. Proc R Soc Lon Ser-A **193:** 120-&.

Perkins, A. K., I. R. Santos, M. Sadat-Noori, J. R. Gatland, and D. T. Maher. 2015. Groundwater seepage as a driver of CO_2 evasion in a coastal lake (Lake Ainsworth, NSW, Australia). Environmental Earth Sciences **74:** 779-792.

Peters, E., G. Bier, H. A. J. van Lanen, and P. J. J. F. Torfs. 2006. Propagation and spatial distribution of drought in a groundwater catchment. Journal of Hydrology **321:** 257-275.

Phillips, C. L., N. Nickerson, D. Risk, and B. J. Bond. 2011. Interpreting diel hysteresis between soil respiration and temperature. Global Change Biology **17:** 515-527.

R-Core-Team. 2016. R: A language and environment for statistical computing. R Foundation for Statistical Computing.

Reichstein, M., F. Bednorz, G. Broll, and T. Kätterer. 2000. Temperature dependence of carbon mineralisation: conclusions from a long-term incubation of subalpine soil samples. Soil Biol. Biochem. **32:** 947-958.

Rey, A. 2015. Mind the gap: non-biological processes contributing to soil CO_2 efflux. Global Change Biology **21:** 1752-1761.

Riveros-Iregui, D. A. and others 2007. Diurnal hysteresis between soil CO_2 and soil temperature is controlled by soil water content. Geophys Res Lett **34**.

Schlesinger, W. H., and J. M. Melack. 1981. Transport of organic carbon in the world's rivers. Tellus **33:** 172-187.

Scholten, M. and others 2005. The River Elbe in Germany - present state, conflicting goals, and perspectives of rehabilitation. Archiv für Hydrobiologie **Suppl. 155:** 579-602.

Spinoni, J., J. V. Vogt, G. Naumann, P. Barbosa, and A. Dosio. 2018. Will drought events become more frequent and severe in Europe? International Journal of Climatology **38:** 1718-1736.

Steward, A. L., D. von Schiller, K. Tockner, J. C. Marshall, and S. E. Bunn. 2012. When the river runs dry: human and ecological values of dry riverbeds. Front. Ecol. Environ. **10:** 202-209.

Tufekcioglu, A., J. W. Raich, T. M. Isenhart, and R. C. Schultz. 2001. Soil respiration within riparian buffers and adjacent crop fields. Plant Soil **229:** 117-124.

UNESCO/IHA. 2010. GHG Measurement Guidlines for Freshwater Reservoirs, p. 138. *In* J. A. Goldenfum [ed.]. UNESCO.

von Schiller, D. and others 2014. Carbon dioxide emissions from dry watercourses. Inland Waters **4:** 377-382.

Weigold, F., and M. Baborowski. 2009. Consequences of delayed mixing for quality assessment of river water: Example Mulde–Saale–Elbe. Journal of Hydrology **369:** 296-304.

Weise, L. and others 2016. Water level changes affect carbon turnover and microbial community composition in lake sediments. FEMS Microbiol. Ecol. **92**.

Wood, W. W., and D. W. Hyndman. 2017. Groundwater Depletion: A Significant Unreported Source of Atmospheric Carbon Dioxide. Earths Future **5:** 1133-1135.

WSV. 2020. ELWIS. Wasserstände & Vorhersagen an schifffahrtsrelevanten Pegeln. Pegel Magdeburg-Strombrücke. Wasserstraßen- und Schifffahrtsverwaltung des Bundes (WSV) im Geschäftsbereich des Bundesministeriums für Verkehr und digitale Infrastruktur (BMVI).

Yvon-Durocher, G. and others 2012. Reconciling the temperature dependence of respiration across timescales and ecosystem types. Nature **487:** 472-476.